Electronic Supplementary Material (ESI) for Journal of Materials Chemistry A.
This journal is © The Royal Society of Chemistry 2021

Supplementary Material

Ultrasensitive Humidity Sensing and their Multifunctional Applications of Borophene-MoS_2 Heterostructures

Chuang Hou, Guoan Tai,* Yi Liu, Zitong Wu, Zenghui Wu and Xinchao Liang

The State Key Laboratory of Mechanics and Control of Mechanical Structures, Key Laboratory for Intelligent Nano Materials and Devices of Ministry of Education, College of Aerospace Engineering, Nanjing University of Aeronautics and Astronautics, Nanjing 210016, China.

Corresponding author: taiguoan@nuaa.edu.cn

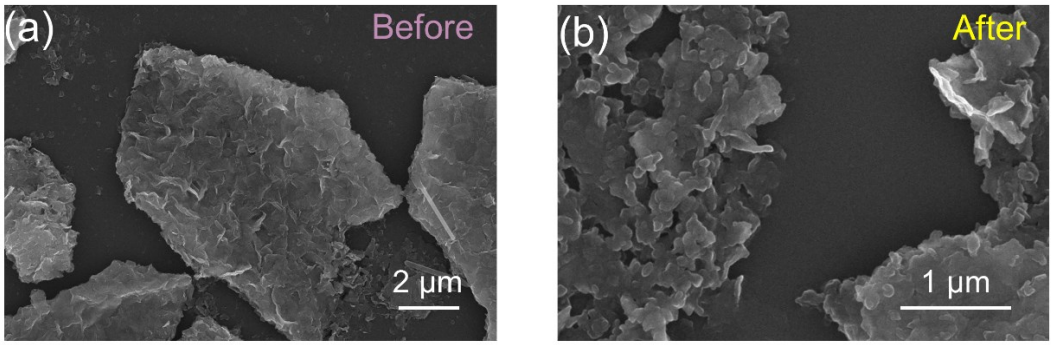

Fig. S1 SEM images of MoS_2 sheets before and after ultrasound.

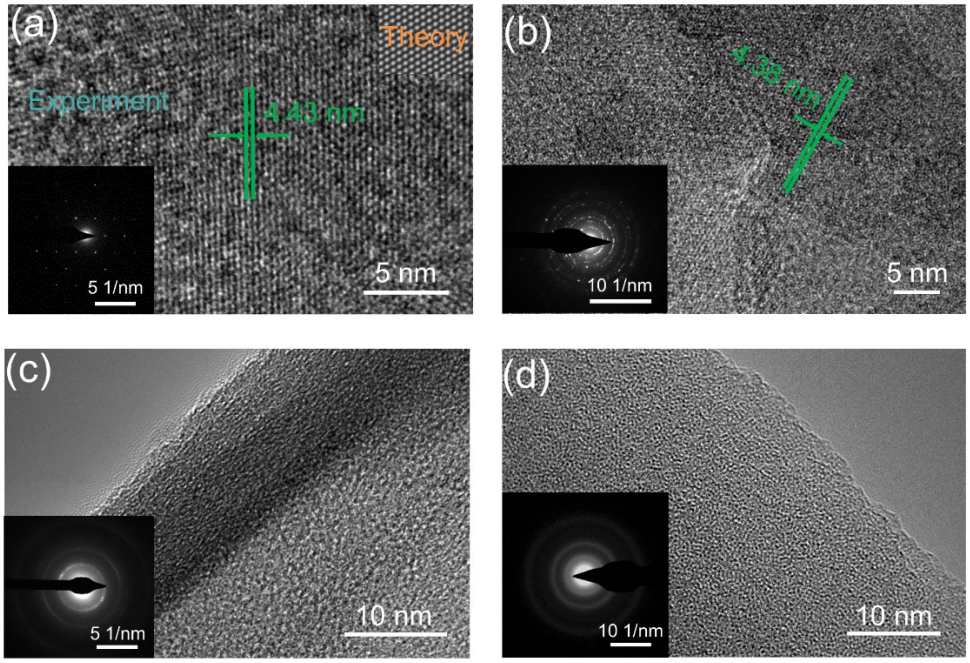

Fig. S2 HRTEM images and SAED patterns of the borophene sheets at 600 ^{o}C for 30 min.

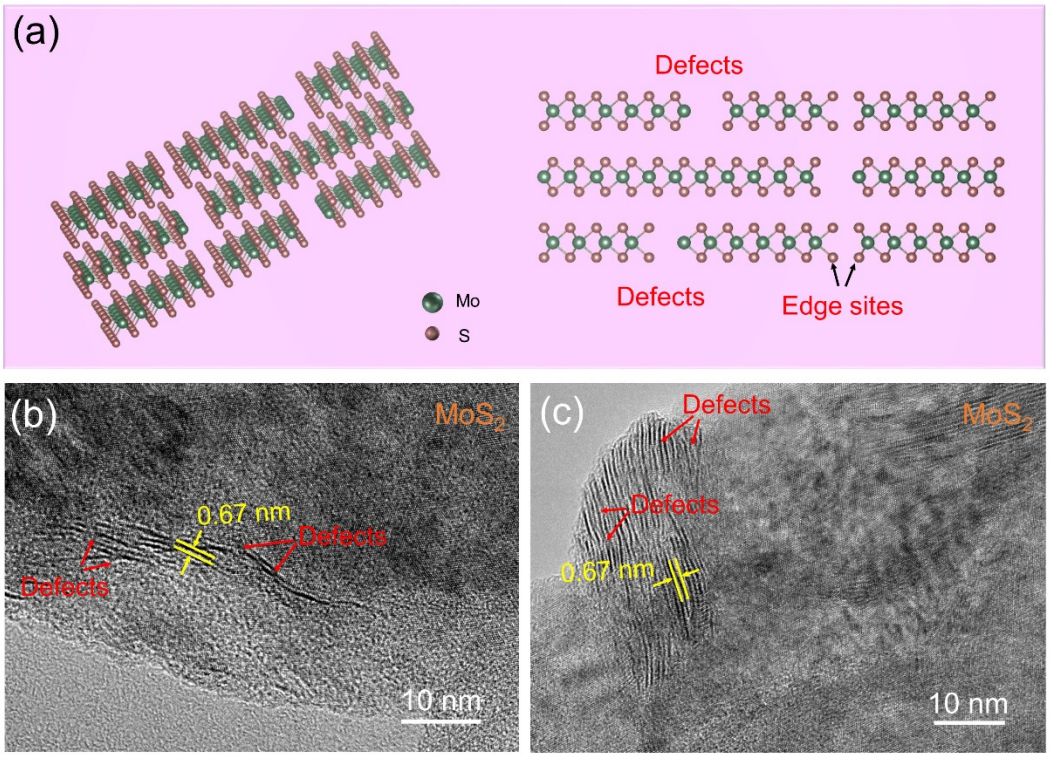

Fig. S3 HRTEM images of the MoS_2 in borophene-MoS_2 heterostructures. (a) Schematic diagram of defective layered MoS_2. (b) HRTEM images of the sheets with many defects.

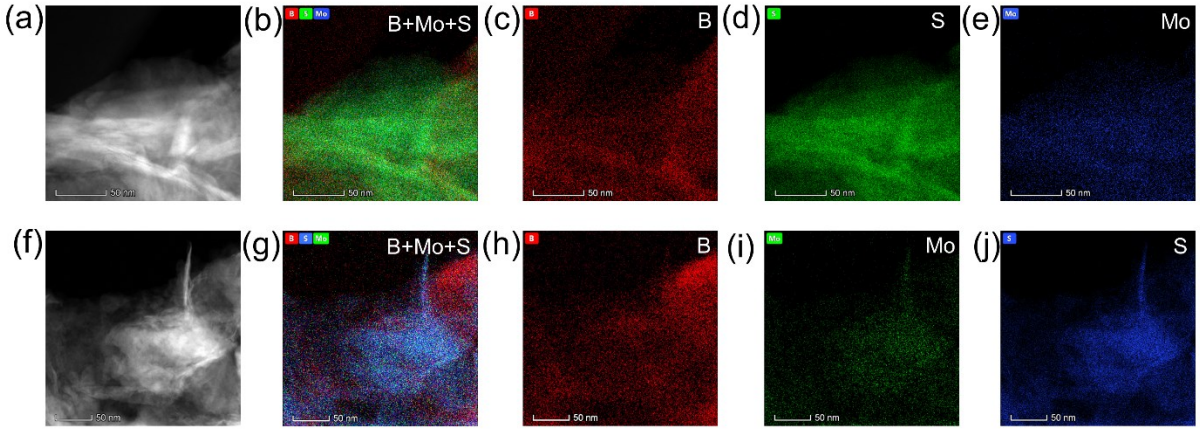

Fig. S4 HAADF-STEM elemental mappings of the heterostructures in different regions.

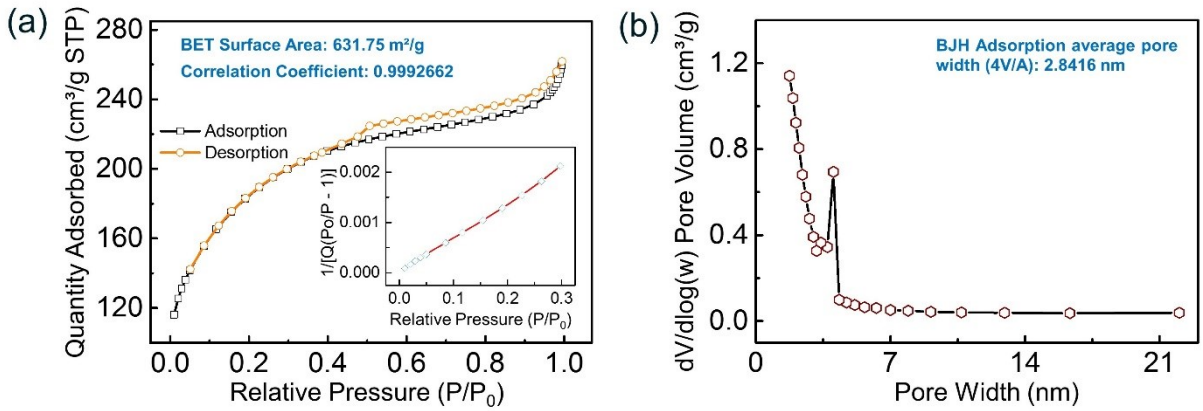

Fig. S5 N_2 adsorption-desorption characteristics of borophene-MoS_2 heterostructures. (a) N_2 adsorption-desorption isotherm. The inset is the corresponding BET surface area plot. (b) Pore-size distribution curve.

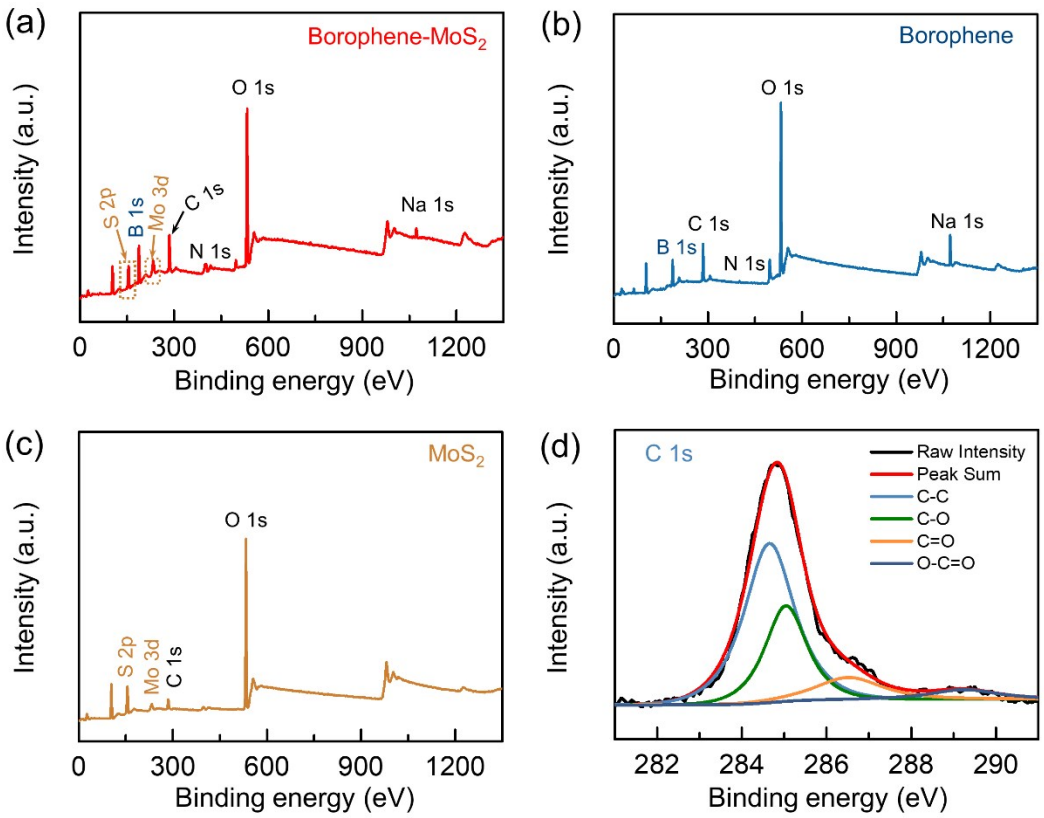

Fig. S6 XPS spectra of borophene-MoS_2 heterostructures, pristine borophene and MoS_2. (a) Full-scale XPS survey of borophene-MoS_2 heterostructures. (b) Full-scale XPS survey of borophene. (c) Full-scale XPS survey of MoS_2. (d) High-resolution C1s spectrum of the heterostructures.

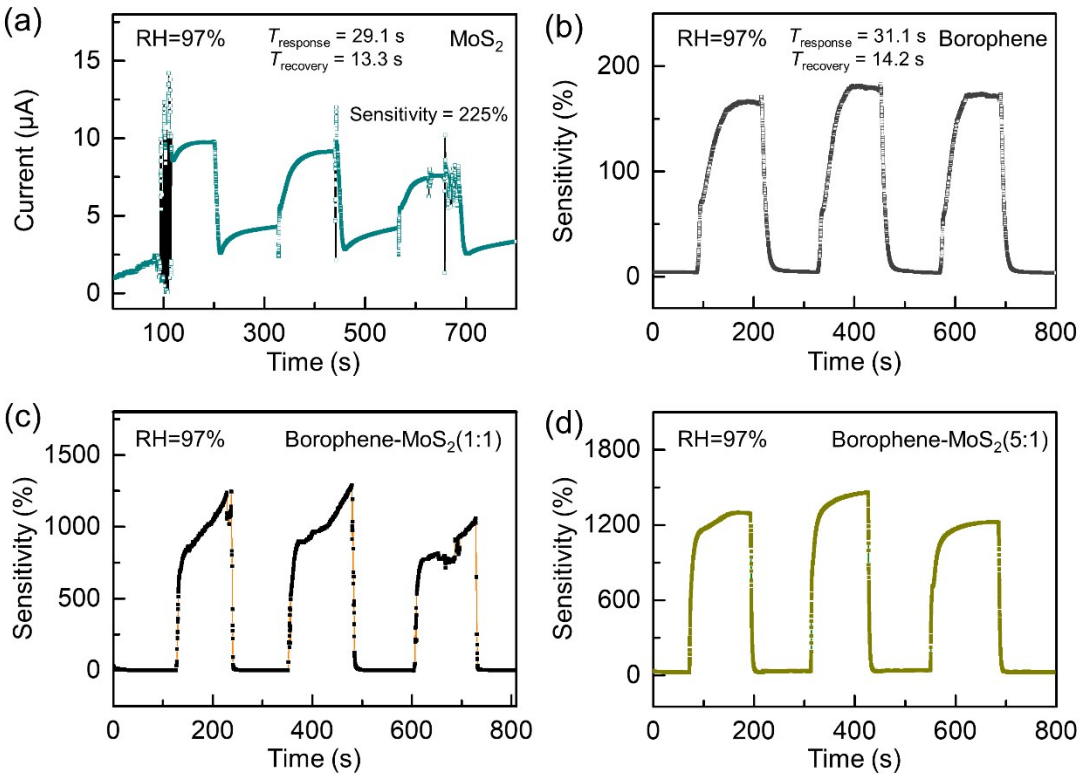

Fig. S7 Response and recovery curves at 97% RH of the sensors based on difference samples: (a) MoS_2, (b) borophene, (c) borophene-MoS_2 (1:1) and (d) borophene-MoS_2 (5:1).

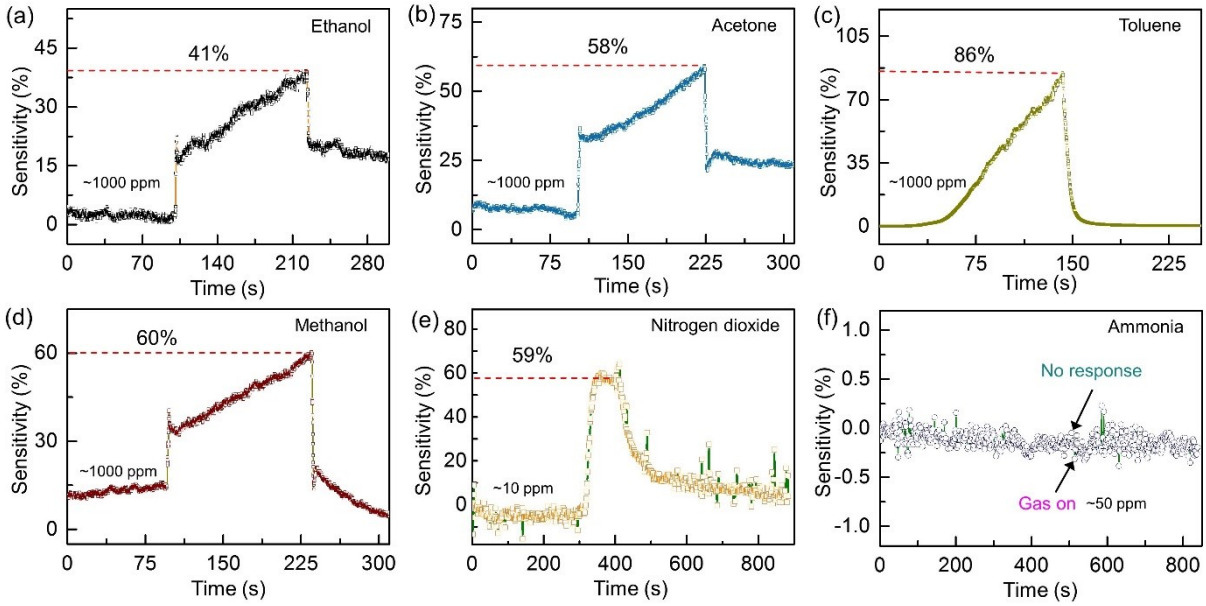

Fig. S8 Response curves of the heterostructured sensor exposed to organic vapors: (a) ethanol, (b) acetone, (c) toluene, (d) methanol, (e) nitrogen dioxide, and (f) ammonia.

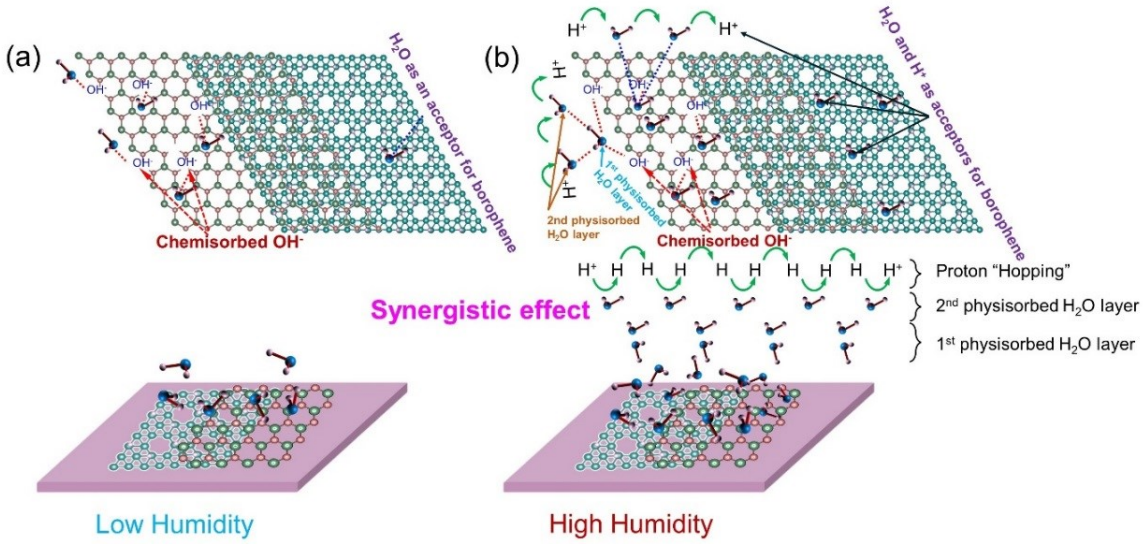

Fig. S9 Schematic diagram of the humidity sensing mechanism of the borophene-MoS_2 heterostructure-based humidity sensor at various humidities: (a) low humidity and (b) high humidity.

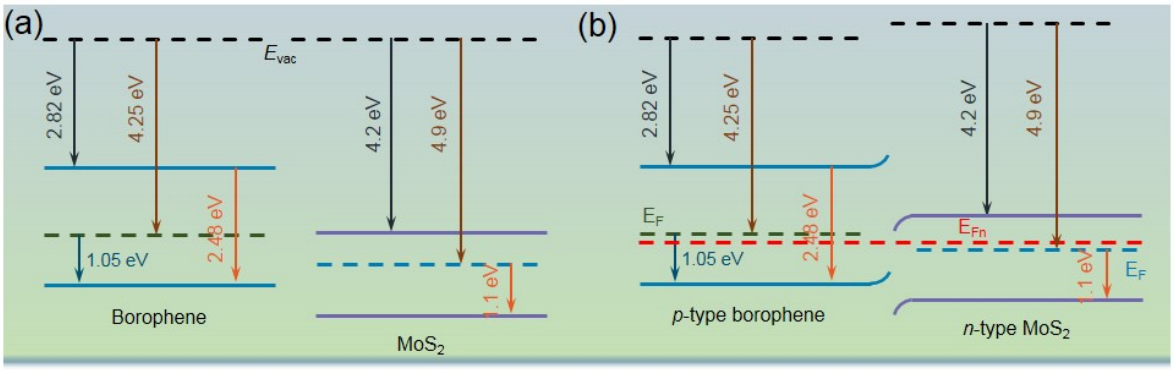

Fig. S10 Band diagrams of borophene and MoS_2 without (a) and with (b) contact.

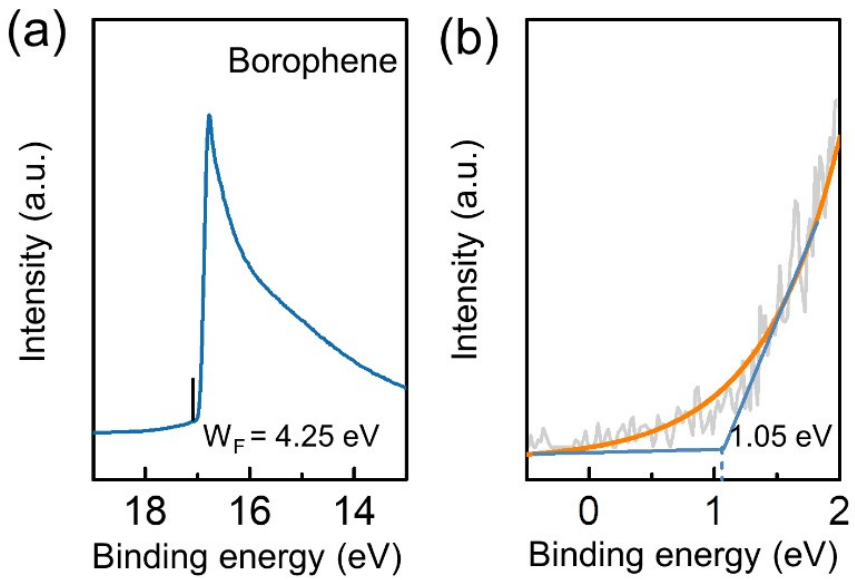

Fig. S11 UPS spectra of borophene. (a) Photoemission cut-off spectra of α′-4H-borophene. (b) Valence band (VB) structure of the borophene.

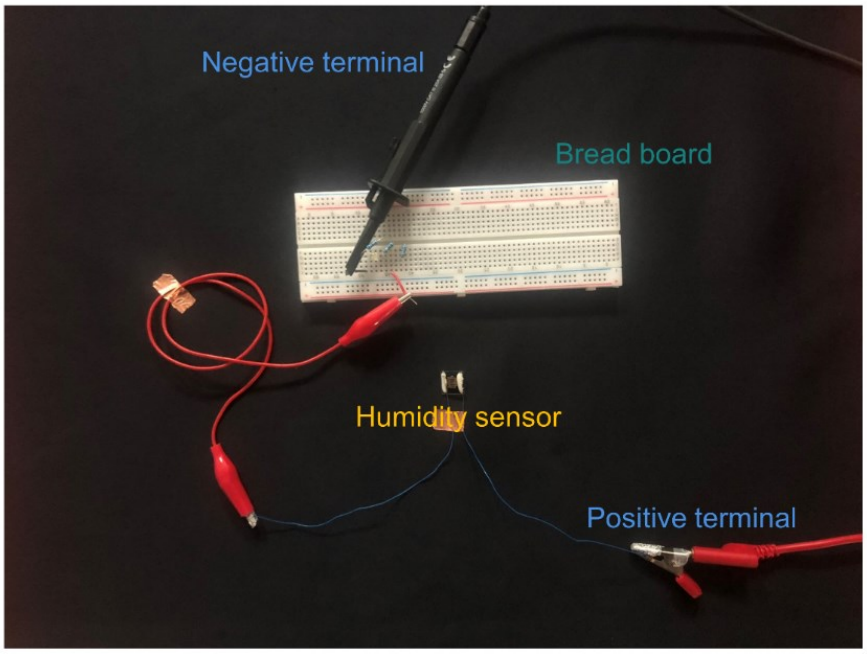

Fig. S12 Photograph of a non-contact humidity switch system.

Calculation of theoretical detection limit

The lowest detection limit of relative humidity can not be obtained by our present experimental setup, the theoretical detection limit is derived from the sensor's signal processing performance. The sensor noise can be calculated by the variation in the relative conductance change in the baseline using the root-mean-square deviation (rmsd).[1-3] The detailed processes are as follows:

Step 1:

We took 10 data points at the baseline in Figure 4b before the exposure of wet vapor.

Time (s)	Current (μA)	$(\Delta I/I)$^1/3 (Yi)
0	0.02896	0.21492
5	0.028613	-0.135461254
10	0.0289	0.195915425
15	0.02891	0.198897398
20	0.0283	0.198897398
25	0.02876	0.138192309
30	0.02816	-0.26341785
35	0.02846	-0.198485296
40	0.029	0.222438577
45	0.02878	0.149424758

Step 2:

After plotting the data, a fifth-order polynomial fit, which gives not only the curve-fitting equation but also the statistical parameters of the polynomial fit, was executed within the data-point range.

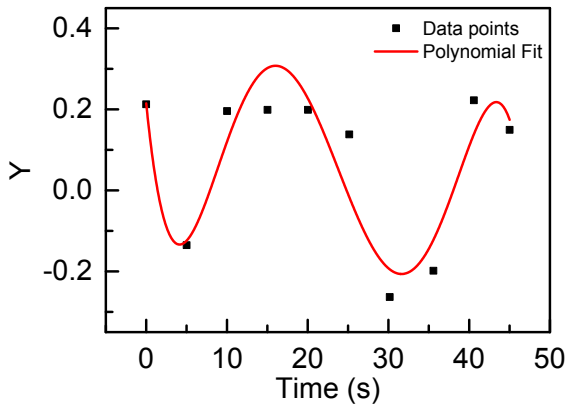

Curve-fitting equation obtained from the fifth order polynomial fit.

Step 3:

The Vχ2 value is then calculated as shown below Vχ2 = Σ (Yi – Y)^2, where Yi is the measured data point and *y* is the corresponding value calculated from the curve-fitting equation.

Time (s)	Yi	Y	$(Yi - Y)^2$
0	0.21492	0.26773	0.002788896
5	-0.135461254	-0.12426	0.000125468
10	0.195915425	0.11984	0.00578747
15	0.198897398	0.30185	0.010599238
20	0.198897398	0.22761	0.000824414
25	0.138192309	-0.00954	0.021824835
30	-0.26341785	-0.19248	0.005032179
35	-0.198485296	-0.14399	0.002969737
40	0.222438577	0.10947	0.012761899
45	0.149424758	0.17411	0.000609361

Step 4:

$rms_{noise} = \sqrt{} (V\chi 2 / N)$ where, N = 10

rmsnoise = 0.079576063

Detection limit: DL (%) = 3 * (rms_{noise} /slope) = 3 * (0.079576063/0.2452) (Slope = 0.2452, the value obtained from Fig. 4c in the text, inset) = 0.9736%

So, the theoretical detection limit calculated is 0.9736%.

References

[1] J. Li, Y. Lu, Q. Ye, M. Cinke, J. Han and M. Meyyappan, *Nano Lett.*, 2003, **3**, 929-933.

[2] V. Dua, S. P. Surwade, S. Ammu, S. R. Agnihotra, S. Jain, K. E. Roberts, S. Park, R. S. Ruoff and S. K. Manohar, *Angew. Chem., Int. Ed.*, 2010, **49**, 2154-2157.

[3] Y. H. Kim, S. J. Kim, Y.-J. Kim, Y.-S. Shim, S. Y. Kim, B. H. Hong and H. W. Jang, *ACS Nano*, 2015, **9**, 10453-10460.